

Demonstration of Monogamy Relations for Einstein-Podolsky-Rosen Steering in Gaussian Cluster States

Xiaowei Deng^{‡,1,2} Yu Xiang^{‡,2,3} Caixing Tian,^{1,2} Gerardo Adesso,⁴ Qiongyi He,^{2,3,*}
Qihuang Gong,^{2,3} Xiaolong Su,^{1,2,†} Changde Xie,^{1,2} and Kunchi Peng^{1,2}

¹State Key Laboratory of Quantum Optics and Quantum Optics Devices,
Institute of Opto-Electronics, Shanxi University, Taiyuan 030006, China

²Collaborative Innovation Center of Extreme Optics, Shanxi University, Taiyuan 030006, China

³State Key Laboratory of Mesoscopic Physics, School of Physics, Peking University,
Collaborative Innovation Center of Quantum Matter, Beijing 100871, China

⁴Centre for the Mathematics and Theoretical Physics of Quantum Non-Equilibrium Systems (CQNE),
School of Mathematical Sciences, The University of Nottingham, Nottingham NG7 2RD, United Kingdom

Understanding how quantum resources can be quantified and distributed over many parties has profound applications in quantum communication. As one of the most intriguing features of quantum mechanics, Einstein-Podolsky-Rosen (EPR) steering is a useful resource for secure quantum networks. By reconstructing the covariance matrix of a continuous variable four-mode square Gaussian cluster state subject to asymmetric loss, we quantify the amount of bipartite steering with a variable number of modes per party, and verify recently introduced monogamy relations for Gaussian steerability, which establish quantitative constraints on the security of information shared among different parties. We observe a very rich structure for the steering distribution, and demonstrate one-way EPR steering of the cluster state under Gaussian measurements, as well as one-to-multi-mode steering. Our experiment paves the way for exploiting EPR steering in Gaussian cluster states as a valuable resource for multipartite quantum information tasks.

Schrödinger [1] put forward the term “steering” to describe the “spooky action-at-a-distance” phenomenon pointed out by Einstein, Podolsky, and Rosen (EPR) in their famous paradox [2, 3]. Wiseman, Jones, and Doherty [4] rigorously defined the concept of steering in terms of violations of local hidden state model, and revealed that steering is an intermediate type of quantum correlation between entanglement [5, 6] and Bell nonlocality [7, 8], where local measurements on one subsystem can apparently adjust (steer) the state of another distant subsystem [9–12]. Such correlation is intrinsically asymmetric with respect to the two subsystems [13–19], and allows verification of shared entanglement even if the measurement devices of one subsystem are untrusted [11]. Due to this intriguing feature, steering has been identified as a physical resource for one-sided device-independent (1sDI) quantum cryptography [20–24], secure quantum teleportation [25–27], and subchannel discrimination [28].

Recently, experimental observation of multipartite EPR steering has been reported in optical networks [29] and photonic qubits [30, 31]. These experiments offer insights into understanding whether and how this special type of quantum correlation can be distributed over many different systems, a problem which has been recently studied theoretically by deriving so-called *monogamy relations* [32–38]. It has been shown that the residual Gaussian steering stemming from a monogamy inequality [36] can act as a quantifier of genuine multipartite steering [39] for pure three-mode Gaussian states, and acquires an operational interpretation in the context of a 1sDI quantum secret sharing protocol [40]. However, beyond [29], no systematic experimental exploration of monogamy constraints for EPR steering has been reported to date.

As generated via an Ising-type interaction, a cluster state features better persistence of entanglement than that of a Greenberger-Horne-Zeilinger (GHZ) state, hence is consid-

ered as a valuable resource for one-way quantum computation [41–45] and quantum communication [46–49]. Continuous variable (CV) cluster states [50, 51], which can be generated deterministically, have been successfully produced for eight [52], 60 [53] and up to 10,000 quantum modes [54]. Several quantum logical operations based on prepared CV cluster states have been experimentally demonstrated [55–58]. While the previous studies of multipartite steering mainly focus on the CV GHZ-like states [59], comparatively little is known about EPR steering and its distribution according to monogamy constraints in CV cluster states.

In this Letter, we experimentally investigate properties of bipartite steering within a CV four-mode square Gaussian cluster state (see Fig. 1), and quantitatively test its monogamy relations [33–37]. By reconstructing the covariance matrix of the cluster state, we measure the quantifier of EPR steering under Gaussian measurements introduced in [15], for various bipartite splits. We find that the two- and three-mode steering properties are determined by the geometric structure of the cluster state. Interestingly, a given mode of the state can be steered by its diagonal mode which is not directly coupled, but can not be steered even by collaboration of its two nearest neighbors, although they are coupled by direct interaction. These properties are different from those of a CV four-mode GHZ-like state. We further present for the first time an experimental observation of a ‘reverse’ steerability, where the party being steered comprises more than one mode. With this ability, we precisely validate four types of monogamy relations recently proposed for Gaussian steering (see Table I) in the presence of loss [33–37]. Our study helps quantify how steering can be distributed among different parties in cluster states and link the amount of steering to the security of channels in a communication network.

The CV cluster quadrature correlations (so-called nullifiers)

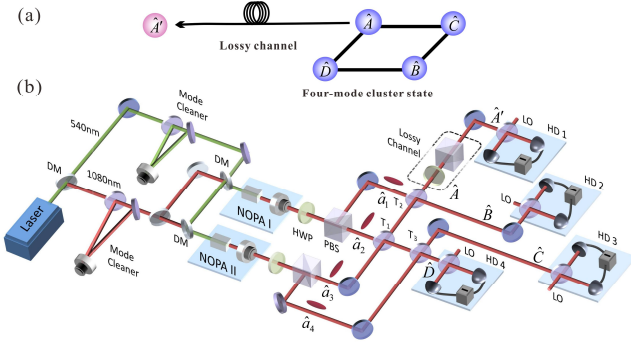


FIG. 1: Scheme of the experiment. (a) An optical mode (\hat{A}) of a four-mode square cluster state is distributed over a lossy quantum channel. (b) The experimental set-up. The squeezed states with -3 dB squeezing at the sideband frequency of 3 MHz are generated from two nondegenerate optical parametric amplifiers (NOPAs). T_1 , T_2 and T_3 are the beam-splitters used to generate the cluster state. The lossy channel is composed by a half-wave plate (HWP) and a polarization beam-splitter (PBS). HD₁₋₄ denote homodyne detectors; LO denotes the local oscillator; and DM denotes dichroic mirror.

can be expressed by [45, 50, 51]

$$(\hat{p}_a - \sum_{b \in N_a} \hat{x}_b) \rightarrow 0, \quad \forall a \in G \quad (1)$$

where $\hat{x}_a = \hat{a} + \hat{a}^\dagger$ and $\hat{p}_a = (\hat{a} - \hat{a}^\dagger)/i$ stand for amplitude and phase quadratures of an optical mode \hat{a} , respectively. The modes of $a \in G$ denote the vertices of the graph G , while the modes of $b \in N_a$ are the nearest neighbors of mode \hat{a} . For an ideal cluster state the left-hand side of Eq. (1) tends to zero, so that the state is a simultaneous zero eigenstate of these quadrature combinations in the limit of infinite squeezing [45].

As a unit of two-dimensional cluster state, a four-mode square cluster state as shown in Fig. 1(a) can be used to establish a quantum network [40, 60]. The cluster state of the optical field is prepared by coupling two phase-squeezed and two amplitude-squeezed states of light on an optical beam-splitter network, which consists of three optical beam-splitters with transmittance of $T_1 = 1/5$ and $T_2 = T_3 = 1/2$, respectively, as shown in Fig. 1(b) [61]. We distribute mode \hat{A} of the state in a lossy channel [Fig. 1(a)]. The output mode is given by

Type	Ref.	Inequality	Specifications
I	[33]	$\mathcal{G}^{A \rightarrow C} > 0 \Rightarrow \mathcal{G}^{B \rightarrow C} = 0$	$n_A = n_B = n_C = 1$
II	[34, 35]	$\mathcal{G}^{A \rightarrow C} > 0 \Rightarrow \mathcal{G}^{B \rightarrow C} = 0$	$n_A, n_B \geq 1; n_C = 1$
IIIa	[36]	$\mathcal{G}^{C \rightarrow (AB)} - \mathcal{G}^{C \rightarrow A} - \mathcal{G}^{C \rightarrow B} \geq 0$	$n_A = n_B = n_C = 1$
IIIb	[36]	$\mathcal{G}^{(AB) \rightarrow C} - \mathcal{G}^{A \rightarrow C} - \mathcal{G}^{B \rightarrow C} \geq 0$	$n_A = n_B = n_C = 1$
IVa	[37]	$\mathcal{G}^{C \rightarrow (AB)} - \mathcal{G}^{C \rightarrow A} - \mathcal{G}^{C \rightarrow B} \geq 0$	$n_A, n_B, n_C \geq 1$
IVb	[37]	$\mathcal{G}^{(AB) \rightarrow C} - \mathcal{G}^{A \rightarrow C} - \mathcal{G}^{B \rightarrow C} \geq 0$	$n_A, n_B \geq 1; n_C = 1$

TABLE I: Classification of monogamy relations for the bipartite quantifier $\mathcal{G}^{j \rightarrow k}$ of EPR steerability of party k by party j under Gaussian measurements, in a tripartite $(n_A + n_B + n_C)$ -mode system ABC . Note: I \sqsubseteq II and III \sqsubseteq IV, where " \sqsubseteq " indicates being generalized by; the relations in types II and IVb can be violated for $n_C > 1$.

$\hat{A}' = \sqrt{\eta}\hat{A} + \sqrt{1-\eta}\hat{v}$, where η and \hat{v} represent the transmission efficiency of the quantum channel and the vacuum mode induced by loss into the quantum channel, respectively.

The properties of a $(n_A + m_B)$ -mode Gaussian state ρ_{AB} of a bipartite system can be determined by its covariance matrix

$$\sigma_{AB} = \begin{pmatrix} A & C \\ C^\top & B \end{pmatrix}, \quad (2)$$

with elements $\sigma_{ij} = \langle \hat{\xi}_i \hat{\xi}_j + \hat{\xi}_j \hat{\xi}_i \rangle / 2 - \langle \hat{\xi}_i \rangle \langle \hat{\xi}_j \rangle$, where $\hat{\xi} \equiv (\hat{x}_1^A, \hat{p}_1^A, \dots, \hat{x}_n^A, \hat{p}_n^A, \hat{x}_1^B, \hat{p}_1^B, \dots, \hat{x}_m^B, \hat{p}_m^B)$ is the vector of the amplitude and phase quadratures of optical modes. The submatrices A and B are corresponding to the reduced states of Alice's and Bob's subsystems, respectively. The partially reconstructed covariance matrix $\sigma_{A'BCD}$, which corresponds to the distributed mode \hat{A}' and modes \hat{B} , \hat{C} and \hat{D} , is measured by four homodyne detectors [61, 66].

The steerability of Bob by Alice ($A \rightarrow B$) for a $(n_A + m_B)$ -mode Gaussian state can be quantified by [15]

$$\mathcal{G}^{A \rightarrow B}(\sigma_{AB}) = \max \left\{ 0, - \sum_{j: \bar{v}_j^{AB|A} < 1} \ln(\bar{v}_j^{AB|A}) \right\}, \quad (3)$$

where $\bar{v}_j^{AB|A}$ ($j = 1, \dots, m_B$) are the symplectic eigenvalues of $\bar{\sigma}_{AB|A} = B - C^\top A^{-1} C$, derived from the Schur complement of A in the covariance matrix σ_{AB} . The quantity $\mathcal{G}^{A \rightarrow B}$ is a monotone under Gaussian local operations and classical communication [37] and vanishes iff the state described by σ_{AB} is nonsteerable by Gaussian measurements [15]. The steerability of Alice by Bob [$\mathcal{G}^{B \rightarrow A}(\sigma_{AB})$] can be obtained by swapping the roles of A and B .

Figure 2 shows a selection of results for the steerability between any two modes [i.e., $(1 + 1)$ -mode partitions] of the cluster state under Gaussian measurements. Surprisingly, as shown in Fig. 2(a) and Fig. S2 in [61], we find that steering does not exist between any two neighboring modes, as one might have expected due to the direct coupling as shown in the definition of cluster state in Eq. (1). Instead, two-mode steering is present between diagonal modes which are not directly coupled, as shown in Fig. 2. This observation can be understood as a consequence of the monogamy relation (type-I) derived from the two-observable (\hat{x} and \hat{p}) EPR criterion [33]: two distinct modes cannot steer a third mode simultaneously by Gaussian measurements. In fact, as shown in Fig. 1, mode \hat{C} and mode \hat{D} are completely symmetric in the cluster state. Thus, if \hat{A}' could be steered by \hat{C} , it should be equally steered by \hat{D} too, which, on the contrary, is forbidden by the type-I monogamy relation. However, there is no such constraint for mode \hat{B} . As a comparison, in a CV GHZ-like state, pairwise steering is strictly forbidden between any two modes based upon the same argument as the state is fully symmetric under mode permutations [32, 67]. Thus, we conclude that a cluster state features richer steerability properties, due to the inherent asymmetry induced by its geometric configuration.

We further investigate quantitatively the robustness of the two-mode steering when transmission loss is imposed on one

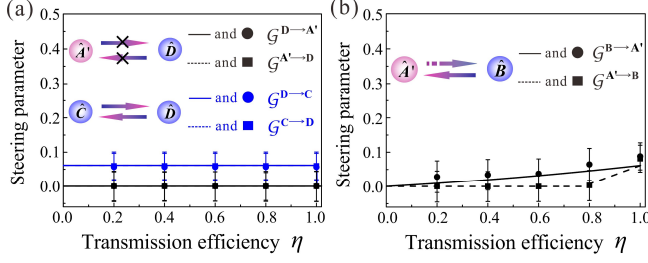


FIG. 2: Gaussian EPR steering between two modes of the cluster state. (a) There is no EPR steering between neighboring modes \hat{A}' and \hat{D} under Gaussian measurements, while diagonal modes \hat{C} and \hat{D} can steer each other with equal power. (b) One-way EPR steering between modes \hat{A}' and \hat{B} under Gaussian measurements. Additional $(1+1)$ -mode partitions are shown in Fig. S2 in [61]. In all the panels, the quantities plotted are dimensionless. The lines and curves represent theoretical predictions based on the theoretical covariance matrix as calculated in [61]. The dots and squares represent the experimental data measured at different transmission efficiencies. Error bars represent \pm one standard deviation and are obtained based on the statistics of the measured noise variances.

of the two parties. In Fig. 2(b), we show the steering parameter defined in Eq. (3) by varying the transmission efficiency η of the lossy channel. When the lossy mode \hat{A}' is the steered party, we find that the non-lossy steering party \hat{B} can always steer \hat{A}' , although the steerability is reduced with increasing loss. However, the presence of loss plays a vital role if \hat{A}' is the steering party. In fact, if the transmission efficiency η is lower than a critical value of ~ 0.772 , the Gaussian steering of \hat{A}' upon \hat{B} is completely destroyed. This leads to a manifestation of “one-way” steering within the region of $\eta \in (0, 0.772)$, as previously noted in other types of entangled states [17–19, 29]. However, we remark that in our experiment we are limited to Gaussian measurements for the steering party, which leaves open the possibility that $A' \rightarrow B$ steering could still be demonstrated for smaller values of η by resorting to suitable non-Gaussian measurements [18, 68].

Since mode \hat{A}' is coupled to its two nearest neighbors \hat{C} and \hat{D} on each side, one may wonder whether the two neighboring modes can jointly steer \hat{A}' . Figures 3 and S3 in [61] show the steerability between one mode and any two other modes of the cluster state [i.e., $(1+2)$ -mode and $(2+1)$ -mode partitions] under Gaussian measurements. Interestingly, we find that mode \hat{A}' still cannot be steered even by the collaboration of modes \hat{C} and \hat{D} ($\mathcal{G}^{CD \rightarrow A'} = 0$) [Fig. 3(a)], but can be steered so long as the diagonal mode \hat{B} is involved ($\mathcal{G}^{BC \rightarrow A'} = \mathcal{G}^{BD \rightarrow A'} > 0$) [Fig. 3(b)]. This phenomenon is determined unambiguously from a generalized monogamy relation applicable to the case of the steering party consisting of an arbitrary number of modes (type-II) [34, 35]. As mode \hat{B} can always steer \hat{A}' [shown in Fig. 2(b)], the other group $\{\hat{C}, \hat{D}\}$ is forbidden to steer the same mode simultaneously. We stress that this property is again in stark contrast to the case of CV four-mode GHZ-like state, where any two modes $\{\hat{i}, \hat{j}\}$ can collectively steer another mode \hat{k} [67] as there is

no two-mode steering to rule out this possibility. Similarly, mode \hat{C} can only be steered by a group comprising the diagonal mode \hat{D} [$\mathcal{G}^{BD \rightarrow C} > 0$ shown in Fig. 3(a), and $\mathcal{G}^{A'D \rightarrow C} > 0$ shown in Fig. 3(c)]. We also show that the collective steerability $\mathcal{G}^{BC(D) \rightarrow A'}$ [solid curve in Fig. 3(b)] is significantly higher than the steerability by \hat{B} mode alone $\mathcal{G}^{B \rightarrow A'}$ [solid curve in Fig. 2(b)], suggesting that although the neighboring modes \hat{C} and \hat{D} cannot steer \hat{A}' by themselves, their roles in assisting collective steering with mode \hat{B} are non-trivial.

We further measure, for the first time, the steerability when the steered party comprises more than one mode, i.e., steering parameters of $(1+2)$ -mode configurations, which are shown in Fig. 3 and in Fig. S3 in [61]. The loss imposed on \hat{A} also leads to asymmetric steerability $\mathcal{G}^{BC \rightarrow A'} \neq \mathcal{G}^{A' \rightarrow BC}$, and a parameter window for one-way steering (under the restriction of Gaussian measurements) with $\eta \in (0, 0.5]$, as shown in Fig. 3(b). In addition, our results $\mathcal{G}^{D \rightarrow BC} > 0$ [$\mathcal{G}^{D \rightarrow BC} = \mathcal{G}^{C \rightarrow BD}$, Fig. 3(a)] and $\mathcal{G}^{A' \rightarrow BC} > 0$ when $\eta > 0.5$ [Fig. 3(b)] also confirm experimentally that, when the steered system is composed of at least two modes, it can be steered by more than one party simultaneously, i.e., the type-II monogamy relation is lifted [35].

Using the results of $(1+2)$ -mode steerability, we also present the first experimental examination of the type-III monogamy relation, called Coffman-Kundu-Wootters (CKW)-type monogamy in reference to the seminal study on monogamy of entanglement [32], which quantifies how the steering is distributed among different subsystems [36]. For a three-mode scenario, the CKW-type monogamy relation reads

$$\mathcal{G}^{k \rightarrow (i,j)}(\sigma_{ijk}) - \mathcal{G}^{k \rightarrow i}(\sigma_{ijk}) - \mathcal{G}^{k \rightarrow j}(\sigma_{ijk}) \geq 0, \quad (4)$$

where $i, j, k \in \{\hat{A}', \hat{B}, \hat{C}, \hat{D}\}$ in our case. We have experimentally verified that this monogamy relation is valid for all possible types of $(1+2)$ -mode steering configurations; some of them are shown in Fig. 3(d).

Next, we study the steerability between one and the remaining three modes within the cluster state, i.e., $(1+3)$ - and $(3+1)$ -mode partitions. As shown in Figs. 4(a), (b), one-way EPR steering (under Gaussian measurements) is observed for bipartitions $(\hat{A}' + \hat{B}\hat{C}\hat{D})$ and $(\hat{B} + \hat{A}'\hat{C}\hat{D})$ when $\eta \leq 0.5$ and $\eta \leq 0.228$, respectively. The asymmetry between the two steering directions for the bipartition $(\hat{C} + \hat{A}'\hat{B}\hat{D})$ grows with increasing transmission efficiency, but no one-way property is observed in this case [Fig. 4(c)], since mode \hat{C} and mode \hat{D} can always steer each other independently. Quantitatively, the $(1+3)$ - and $(3+1)$ -mode steerability degrees are further enhanced in comparison to the $(1+2)$ and $(2+1)$ mode cases, even when the newly added mode alone cannot steer or be steered by the other party. We also confirm that the generalized CKW-type monogamy inequality $\mathcal{G}^{k \rightarrow (i,j,l)} - \mathcal{G}^{k \rightarrow i} - \mathcal{G}^{k \rightarrow j} - \mathcal{G}^{k \rightarrow l} \geq 0$ holds in this four-mode scenario, as shown in Fig. 4(d).

Finally, our experiment also validates for the first time general monogamy inequalities for Gaussian steerability with an arbitrary number of modes per party (type-IV) [37]. As a typical example of $(2+2)$ -mode steering, our experimental results demonstrate that the steerability of $(\hat{A}'\hat{B} + \hat{C}\hat{D})$ -mode parti-

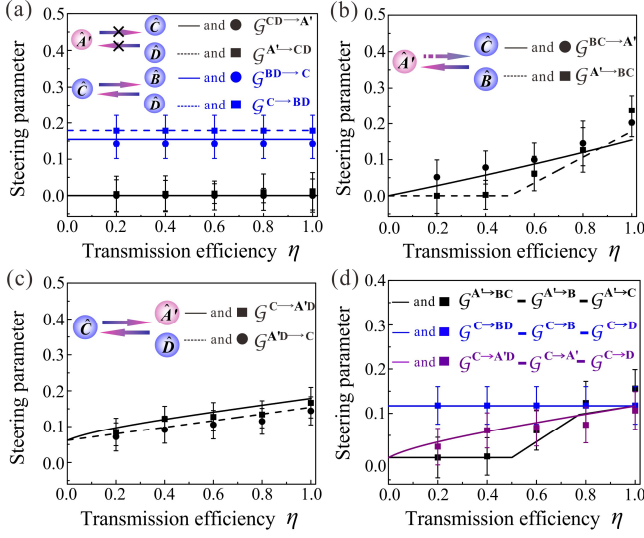


FIG. 3: Gaussian EPR steering between one and two modes of the cluster state. (a) Mode \hat{A}' cannot be steered by the collaboration of two nearest neighboring modes $\{\hat{C}, \hat{D}\}$ even though they are directly coupled; while \hat{C} and $\{\hat{B}, \hat{D}\}$ can steer each other. (b) One-way EPR steering between modes \hat{A}' and $\{\hat{B}, \hat{C}\}$ under Gaussian measurements. (c) \hat{C} and $\{\hat{A}', \hat{D}\}$ can steer each other asymmetrically and the steerability grows with increasing transmission efficiency, reflecting the different effect when loss happens on steering or steered channel. (d) Validation of CKW-type monogamy for steering (type-III). Additional partitions are shown in Fig. S3 in [61]. In all the panels, the quantities plotted are dimensionless. The lines and curves represent theoretical predictions based on the theoretical covariance matrix as calculated in [61]. The dots and squares represent the experimental data measured at different transmission efficiencies. Error bars represent \pm one standard deviation and are obtained based on the statistics of the measured noise variances.

tions satisfies the following inequalities

$$\mathcal{G}^{A'B \rightarrow CD} - \mathcal{G}^{A'B \rightarrow C} - \mathcal{G}^{A'B \rightarrow D} \geq 0, \quad (5a)$$

$$\mathcal{G}^{CD \rightarrow A'B} - \mathcal{G}^{C \rightarrow A'B} - \mathcal{G}^{D \rightarrow A'B} \geq 0, \quad (5b)$$

as indicated in Fig. 4(d). We have verified that both these monogamy relations are also valid for all possible (2 + 2)-mode configurations in this cluster state. Note that, in general, Eq. (5b) can be violated on other classes of states [37].

In summary, the structure and sharing of EPR steering distributed over two-, three-, and four-mode partitions have been demonstrated and investigated quantitatively for a CV four-mode square Gaussian cluster state subject to asymmetric loss. By generating the cluster state deterministically and reconstructing its covariance matrix, we obtain a full steering characterization for all bipartite configurations. For general cases with arbitrary numbers of modes in each party, we quantify the bipartite steerability by Gaussian measurements, and provide experimental confirmation for four types of monogamy relations which bound the distribution of steerability among different modes, as summarized in Table I. Even though our state does not display genuine multipartite steering [39], several innovative features are observed, including the

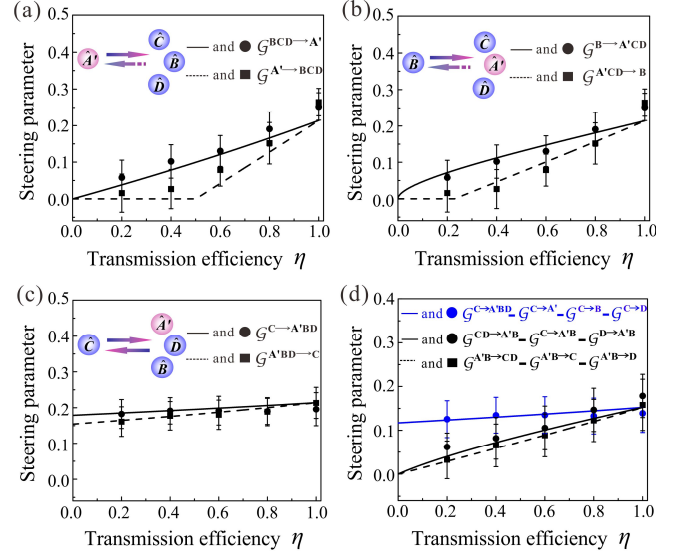


FIG. 4: Gaussian EPR steering between one and three modes in the cluster state. (a) One-way EPR steering under Gaussian measurements between modes \hat{A}' and $\{\hat{B}, \hat{C}, \hat{D}\}$ with directional property. (b) One-way EPR steering under Gaussian measurements between modes \hat{B} and $\{\hat{A}', \hat{C}, \hat{D}\}$. (c) Asymmetric steering between modes \hat{C} and $\{\hat{A}', \hat{B}, \hat{D}\}$. (d) Monogamy of steering quantifier for (1 + 3)- and (2 + 2)-mode partitions. In all the panels, the quantities plotted are dimensionless. The lines and curves represent theoretical predictions based on the theoretical covariance matrix as calculated in [61]. The dots and squares represent the experimental data measured at different transmission efficiencies. Error bars represent \pm one standard deviation and are obtained based on the statistics of the measured noise variances.

steerability of a group of two or three modes by a single mode, and the fact that a given mode of the state can be steered by its diagonal mode which is not directly coupled, but can not be jointly steered by its two directly coupled nearest neighbors.

Our work thus provides a concrete in-depth understanding of EPR steering and its monogamy in paradigmatic multipartite states such as cluster states. In turn, this can be useful to gauge the usefulness of these states for quantum communication technologies. For instance, secure CV teleportation with fidelity exceeding the no-cloning threshold requires two-way Gaussian steering [26], which arises in various partitions in our state, e.g. between \hat{A}' and \hat{B} for sufficiently large transmission efficiency [see Fig. 2(b)]. Furthermore, the amount of Gaussian steering directly bounds the secure key rate in CV 1sDI quantum key distribution and secret sharing [22, 36, 40]. Combined with a stronger initial squeezing level, the techniques used here could be adapted to demonstrate these protocols among many sites over lossy quantum channels.

This research was supported by National Natural Science Foundation of China (Grants No. 11522433, No. 11622428, No. 61475092, and No. 61475006), Ministry of Science and Technology of China (Grants No. 2016YFA0301402 and No. 2016YFA0301302), X. Su thanks the program of Youth Sanjin Scholar, Q. He thanks the Cheung Kong Scholars Programme

(Youth) of China, GA thanks the European Research Council (ERC) Starting Grant GQCOP (Grant No. 637352) and the Foundational Questions Institute (fqxi.org) Physics of the Observer Programme (Grant No. FQXi-RFP-1601).

[‡]X. Deng and Y. Xiang contributed equally to this work.

* Electronic address: qiongyihe@pku.edu.cn

† Electronic address: suxl@sxu.edu.cn

- [1] E. Schrödinger, “Discussion of probability relations between separated systems,” *Proc. Cambridge Philos. Soc.* **31**, 555–563 (1935).
- [2] A. Einstein, B. Podolsky, and N. Rosen, “Can quantum-mechanical description of physical reality be considered complete?” *Phys. Rev.* **47**, 777–780 (1935).
- [3] M. D. Reid, “Demonstration of the Einstein-Podolsky-Rosen paradox using nondegenerate parametric amplification,” *Phys. Rev. A* **40**, 913–923 (1989).
- [4] H. M. Wiseman, S. J. Jones, and A. C. Doherty, “Steering, entanglement, nonlocality, and the Einstein-Podolsky-Rosen paradox,” *Phys. Rev. Lett.* **98**, 140402 (2007).
- [5] E. Schrödinger, “Die gegenwärtige Situation in der Quantenmechanik,” *Die Naturwissenschaften* **23**, 823–828 (1935).
- [6] R. Horodecki, P. Horodecki, M. Horodecki, and K. Horodecki, “Quantum entanglement,” *Rev. Mod. Phys.* **81**, 865–942 (2009).
- [7] J. S. Bell, “On the Einstein Podolsky Rosen paradox,” *Physics* **1**, 195–200 (1964).
- [8] N. Brunner, D. Cavalcanti, S. Pironio, V. Scarani, and S. Wehner, “Bell nonlocality,” *Rev. Mod. Phys.* **86**, 419–478 (2014).
- [9] S. J. Jones, H. M. Wiseman, and A. C. Doherty, “Entanglement, Einstein-Podolsky-Rosen correlations, Bell nonlocality, and steering,” *Phys. Rev. A* **76**, 052116 (2007).
- [10] M. D. Reid, P. D. Drummond, W. P. Bowen, E. G. Cavalcanti, P. K. Lam, H. A. Bachor, U. L. Andersen, and G. Leuchs, “Colloquium: The Einstein-Podolsky-Rosen paradox: From concepts to applications,” *Rev. Mod. Phys.* **81**, 1727–1751 (2009).
- [11] E. G. Cavalcanti, S. J. Jones, H. M. Wiseman, and M. D. Reid, “Experimental criteria for steering and the Einstein-Podolsky-Rosen paradox,” *Phys. Rev. A* **80**, 032112 (2009).
- [12] D. Cavalcanti and P. Skrzypczyk, “Quantum steering: a review with focus on semidefinite programming,” *Rep. Prog. Phys.* **80**, 024001 (2017).
- [13] S. L. W. Midgley, A. J. Ferris, and M. K. Olsen, *Phys. Rev. A* **81**, 022101 (2010); S. P. Walborn, A. Salles, R. M. Gomes, F. Toscano, and P. H. Souto Ribeiro, *Phys. Rev. Lett.* **106**, 130402 (2011); J. Schneeloch, C. J. Broadbent, S. P. Walborn, E. G. Cavalcanti, and J. C. Howell, *Phys. Rev. A* **87**, 062103 (2013); J. Bowles, T. Vertesi, M. T. Quintino, and N. Brunner, *Phys. Rev. Lett.* **112**, 200402 (2014); B. Opanchuk, L. Arnaud, and M. D. Reid, *Phys. Rev. A* **89**, 062101 (2014).
- [14] Q. Y. He, Q. H. Gong, and M. D. Reid, “Classifying directional Gaussian entanglement, Einstein-Podolsky-Rosen steering, and discord,” *Phys. Rev. Lett.* **114**, 060402 (2015).
- [15] I. Kogias, A. R. Lee, S. Ragy, and G. Adesso, “Quantification of Gaussian quantum steering,” *Phys. Rev. Lett.* **114**, 060403 (2015).
- [16] L. Rosales-Zárate, R. Y. Teh, S. Kiesewetter, A. Brolis, K. Ng, and M. D. Reid, “Decoherence of Einstein-Podolsky-Rosen steering,” *J. Opt. Soc. Am. B* **32**, A82–A91 (2015).
- [17] V. Händchen, T. Eberle, S. Steinlechner, A. Sambrowski, T. Franz, R. F. Werner, and R. Schnabel, “Observation of one-way Einstein-Podolsky-Rosen steering,” *Nat. Photonics* **6**, 596–599 (2012).
- [18] S. Wollmann, N. Walk, A. J. Bennet, H. M. Wiseman, and G. J. Pryde, “Observation of genuine one-way Einstein-Podolsky-Rosen steering,” *Phys. Rev. Lett.* **116**, 160403 (2016).
- [19] K. Sun, X. J. Ye, J. S. Xu, X. Y. Xu, J. S. Tang, Y. C. Wu, J. L. Chen, C. F. Li, and G. C. Guo, “Experimental quantification of asymmetric Einstein-Podolsky-Rosen steering,” *Phys. Rev. Lett.* **116**, 160404 (2016).
- [20] M. Tomamichel and R. Renner, “Uncertainty relation for smooth entropies,” *Phys. Rev. Lett.* **106**, 110506 (2011).
- [21] C. Branciard, E. G. Cavalcanti, S. P. Walborn, V. Scarani, and H. M. Wiseman, “One-sided device-independent quantum key distribution: security, feasibility, and the connection with steering,” *Phys. Rev. A* **85**, 010301 (2012).
- [22] N. Walk, S. Hosseini, J. Geng, O. Thearle, J. Y. Haw, S. Armstrong, S. M. Assad, J. Janousek, T. C. Ralph, T. Symul, H. M. Wiseman, and P. K. Lam, “Experimental demonstration of Gaussian protocols for one-sided device-independent quantum key distribution,” *Optica* **3**, 634–642 (2016).
- [23] T. Gehring, V. Händchen, J. Duhme, F. Furrer, T. Franz, C. Pacher, R. F. Werner, and R. Schnabel, “Implementation of continuous-variable quantum key distribution with composable and one-sided-device independent security against coherent attacks,” *Nat. Commun.* **6**, 8795 (2015).
- [24] R. Gallego, and L. Aolita, “Resource theory of steering,” *Phys. Rev. X* **5**, 041008 (2015).
- [25] M. D. Reid, “Signifying quantum benchmarks for qubit teleportation and secure quantum communication using Einstein-Podolsky-Rosen steering inequalities,” *Phys. Rev. A*, **88**, 062338 (2013).
- [26] Q. He, L. Rosales-Zárate, G. Adesso, and M. D. Reid, “Secure continuous variable teleportation and Einstein-Podolsky-Rosen steering,” *Phys. Rev. Lett.* **115**, 180502 (2015).
- [27] C.-Y. Chiu, N. Lambert, Teh-Lu Liao, F. Nori, and C.-M. Li, “No-cloning of quantum steering,” *NPJ Quantum Information* **2**, 16020 (2016).
- [28] M. Piani and J. Watrous, “Necessary and sufficient quantum information characterization of Einstein-Podolsky-Rosen steering,” *Phys. Rev. Lett.* **114**, 060404 (2015).
- [29] S. Armstrong, M. Wang, R. Y. Teh, Q. H. Gong, Q. Y. He, J. Janousek, H. A. Bachor, M. D. Reid, and P. K. Lam, “Multipartite Einstein-Podolsky-Rosen steering and genuine tripartite entanglement with optical networks,” *Nat. Phys.* **11**, 167–172 (2015).
- [30] D. Cavalcanti, P. Skrzypczyk, G. H. Aguilar, R. V. Nery, P. H. Souto Ribeiro, and S. P. Walborn, “Detection of entanglement in asymmetric quantum networks and multipartite quantum steering,” *Nat. Commun.*, **6**, 7941 (2015).
- [31] C.-M. Li, K. Chen, Y.-N. Chen, Q. Zhang, Y.-A. Chen, and J.-W. Pan, “Genuine high-order Einstein-Podolsky-Rosen steering,” *Phys. Rev. Lett.*, **115**, 010402 (2015).
- [32] V. Coffman, J. Kundu, and W. K. Wootters, “Distributed entanglement,” *Phys. Rev. A* **61**, 052306 (2000).
- [33] M. D. Reid, “Monogamy inequalities for the Einstein-Podolsky-Rosen paradox and quantum steering,” *Phys. Rev. A* **88**, 062108 (2013).
- [34] S.-W. Ji, M. S. Kim and H. Nha, “Quantum steering of multimode Gaussian states by Gaussian measurements: Monogamy relations and the Peres conjecture,” *J. Phys. A: Math. Theor.* **48**, 135301 (2015).
- [35] G. Adesso and R. Simon, “Strong subadditivity for log-determinant of covariance matrices and its applications,” *J. Phys. A: Math. Theor.* **49**, 34LT02 (2016).

- [36] Y. Xiang, I. Kogias, G. Adesso, and Q. Y. He, “Multipartite Gaussian steering: monogamy constraints and quantum cryptography applications,” *Phys. Rev. A* **95**, 010101(R) (2017).
- [37] L. Lami, C. Hirche, G. Adesso, and A. Winter, “Schur complement inequalities for covariance matrices and monogamy of quantum correlations,” *Phys. Rev. Lett.* **117**, 220502 (2016).
- [38] S. Cheng, A. Milne, M. J. W. Hall, and H. M. Wiseman, “Volume monogamy of quantum steering ellipsoids for multiqubit systems,” *Phys. Rev. A* **94**, 042105 (2016).
- [39] Q. Y. He and M. D. Reid, “Genuine multipartite Einstein-Podolsky-Rosen steering,” *Phys. Rev. Lett.* **111**, 250403 (2013).
- [40] I. Kogias, Y. Xiang, Q. Y. He, and G. Adesso, “Unconditional security of entanglement-based continuous variable quantum secret sharing,” *Phys. Rev. A* **95**, 012315 (2017).
- [41] R. Raussendorf, and H. J. Briegel, “A one-way quantum computer,” *Phys. Rev. Lett.* **86**, 5188-5191 (2001).
- [42] P. Walther, K. J. Resch, T. Rudolph, E. Schenck, H. Weinfurter, V. Vedral, M. Aspelmeyer, and A. Zeilinger, “Experimental one-way quantum computing,” *Nature* **434**, 169–176 (2005).
- [43] N. C. Menicucci, P. van Loock, M. Gu, C. Weedbrook, T. C. Ralph, and M. A. Nielsen, “Universal quantum computation with continuous-variable cluster states,” *Phys. Rev. Lett.* **97**, 110501 (2006).
- [44] P. van Loock, “Examples of Gaussian cluster computation,” *J. Opt. Soc. Am. B.* **24**, 340–346 (2007).
- [45] M. Gu, C. Weedbrook, N. C. Menicucci, T. C. Ralph, and P. van Loock, “Quantum computing with continuous-variable clusters,” *Phys. Rev. A* **79**, 062318 (2009).
- [46] J. Zhang, G. Adesso, C. Xie, and K. Peng, “Quantum teamwork for unconditional multiparty communication with Gaussian states” *Phys. Rev. Lett.* **103**, 070501 (2009).
- [47] S. Muralidharan and P. K. Panigrahi, “Quantum-information splitting using multipartite cluster states,” *Phys. Rev. A* **78**, 062333 (2008).
- [48] Y. Qian, Z. Shen, G. He, and G. Zeng, “Quantum-cryptography network via continuous-variable graph states,” *Phys. Rev. A* **86**, 052333 (2012).
- [49] H.-K. Lau and C. Weedbrook, “Quantum secret sharing with continuous-variable cluster states,” *Phys. Rev. A* **88**, 042313 (2013).
- [50] J. Zhang and S. L. Braunstein, “Continuous-variable Gaussian analog of cluster state,” *Phys. Rev. A* **73**, 032318 (2006).
- [51] P. van Loock, C. Weedbrook, and M. Gu, “Building Gaussian cluster states by linear optics,” *Phys. Rev. A* **76**, 032321 (2007).
- [52] X. L. Su, Y. P. Zhao, S. H. Hao, *et al.* “Experimental preparation of eight-partite cluster state for photonic qumodes,” *Opt. Lett.* **37**, 5178-5180 (2012).
- [53] M. Chen, N. C. Menicucci, and O. Pfister, “Experimental realization of multipartite entanglement of 60 modes of a quantum optical frequency comb,” *Phys. Rev. Lett.* **112**, 120505 (2014).
- [54] S. Yokoyama, R. Ukai, S. C. Armstrong, C. Sornphiphatphong, T. Kaji, S. Suzuki, J.-i. Yoshikawa, H. Yonezawa, N. C. Menicucci, and A. Furusawa “Optical generation of ultra-large-scale continuous-variable cluster states,” *Nature Photon.* **7**, 982-986 (2013).
- [55] Y. Wang, X. Su, H. Shen, A. Tan, C. Xie, and K. Peng, “Toward demonstrating controlled-X operation based on continuous-variable four-partite cluster states and quantum teleporters,” *Phys. Rev. A* **81**, 022311 (2010).
- [56] R. Ukai, N. Iwata, Y. Shimokawa, S. C. Armstrong, A. Politi, J. -i. Yoshikawa, P. van Loock, and A. Furusawa, “Demonstration of unconditional one-way quantum computations for continuous variables,” *Phys. Rev. Lett.* **106**, 240504 (2011).
- [57] R. Ukai, S. Yokoyama, J. I. Yoshikawa, P. van Loock, and A. Furusawa, “Demonstration of unconditional one-way quantum computations for continuous variables,” *Phys. Rev. Lett.* **107**, 250501 (2011).
- [58] X. Su, S. Hao, X. Deng, L. Ma, M. Wang, X. Jia, C. Xie, and K. Peng, “Gate sequence for continuous variable one-way quantum computation,” *Nat. Commun.* **4**, 2828-2836 (2013).
- [59] P. van Loock and S. L. Braunstein, “Multipartite entanglement for continuous variables: A quantum teleportation network,” *Phys. Rev. Lett.* **84**, 3482 (2000); P. van Loock and S. L. Braunstein, “Greenberger-Horne-Zeilinger nonlocality in phase space,” *Phys. Rev. A* **63**, 022106 (2001).
- [60] H. Shen, X. Su, X. Jia, and C. Xie, “Quantum communication network utilizing quadripartite entangled states of optical field,” *Phys. Rev. A* **80**, 042320 (2009).
- [61] See Supplemental Material for details of the experimental setup, preparation and verification of the cluster state, measurement of the covariance matrix, and additional figures. The Supplemental Material contains additional references [62–65].
- [62] Y. Zhou, X. Jia, F. Li, C. Xie, and K. Peng, “Experimental generation of 8.4 dB entangled state with an optical cavity involving a wedged type-II nonlinear crystal,” *Opt. Express*, **23**, 4952-4959 (2015).
- [63] X. Su, A. Tan, X. Jia, J. Zhang, C. Xie, and K. Peng, “Experimental preparation of quadripartite cluster and Greenberger-Horne-Zeilinger entangled states for continuous variables,” *Phys. Rev. Lett.* **98**, 070502 (2007).
- [64] G. Adesso and F. Illuminati, “Entanglement in continuous-variable systems: recent advances and current perspectives,” *J. Phys. A: Math. Theor.* **40**, 7821 (2007).
- [65] P. van Loock and A. Furusawa, “Detecting genuine multipartite continuous-variable entanglement,” *Phys. Rev. A* **67**, 052315 (2003).
- [66] S. Steinlechner, J. Bauchrowitz, T. Eberle, R. Schnabel, “Strong Einstein-Podolsky-Rosen steering with unconditional entangled states,” *Phys. Rev. A* **87**, 022104 (2013).
- [67] M. Wang, Y. Xiang, Q. Y. He, and Q. H. Gong, “Detection of quantum steering in multipartite continuous-variable Greenberger-Horne-Zeilinger-like states,” *Phys. Rev. A* **91**, 012112 (2015).
- [68] S.-W. Ji, J. Lee, J. Park, and H. Nha, “Quantum steering of Gaussian states via non-Gaussian measurements,” *Sci. Rep.* **6**, 29729 (2016).

Supplemental Material

Details of the experimental setup

In the experiment, the \hat{x} -squeezed and \hat{p} -squeezed states are produced by non-degenerate optical parametric amplifiers (NOPAs) pumped by a common laser source, which is a continuous wave intracavity frequency-doubled and frequency-stabilized Nd:YAP-LBO (Nd-doped YAlO₃ perovskite-lithium triborate) laser. Two mode cleaners are inserted between the laser source and the NOPAs to filter noise and higher order spatial modes of the laser beams at 540 nm and 1080 nm, respectively. The fundamental wave at 1080 nm wavelength is used for the injected signals of NOPAs and the local oscillators of homodyne detectors. The second-harmonic wave at 540 nm wavelength serves as the pump field of the NOPAs, in which through an intracavity frequency-down-conversion process a pair of signal and idler modes with the identical fre-

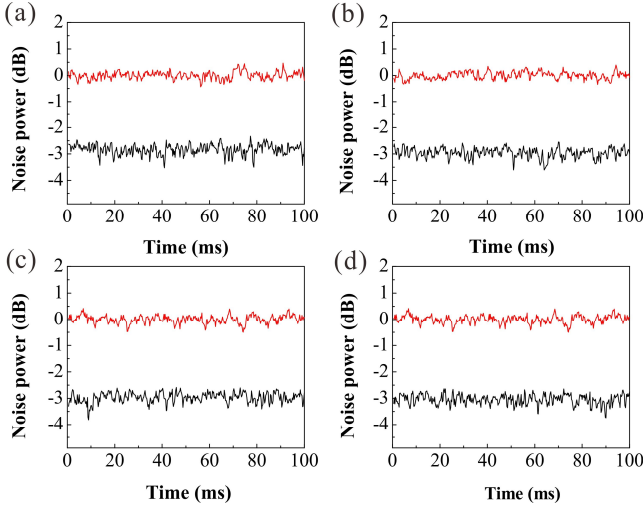


FIG. S1: The experimentally measured quantum correlation variances of the original CV four-mode square Gaussian cluster state. Panels (a)–(d) show the noise powers of $\Delta^2(\hat{p}_A - \hat{x}_C - \hat{x}_D)$, $\Delta^2(\hat{p}_B - \hat{x}_C - \hat{x}_D)$, $\Delta^2(\hat{p}_C - \hat{x}_A - \hat{x}_B)$ and $\Delta^2(\hat{p}_D - \hat{x}_A - \hat{x}_B)$, respectively. The red and black lines are the normalized shot-noise-level and correlated noise, respectively. The measurement frequency is 3 MHz, the resolution bandwidth of the spectrum analyser is 30 KHz, and the video bandwidth of the spectrum analyser is 300 Hz.

quency at 1080 nm and the orthogonal polarizations are generated.

Each of NOPAs consists of an α -cut type-II KTiOPO4 (KTP) crystal and a concave mirror. The front face of KTP crystal is coated to be used for the input coupler and the concave mirror serves as the output coupler of squeezed states, which is mounted on a piezo-electric transducer for locking actively the cavity length of NOPAs on resonance with the injected signal at 1080 nm. The transmissivities of the front face of KTP crystal at 540 nm and 1080 nm are 21.2% and 0.04%, respectively. The end-face of KTP is cut to 1° along y-z plane of the crystal and is antireflection coated for both 1080 nm and 540 nm [62]. The transmissivities of output coupler at 540 nm and 1080 nm are 0.5% and 12.5%, respectively. In our experiment, all NOPAs are operated at the parametric deamplification situation [62, 63]. Under this condition, the coupled modes at $+45^\circ$ and -45° polarization directions are the \hat{x} -squeezed and \hat{p} -squeezed states, respectively [63]. The quantum efficiency of the photodiodes used in the homodyne detectors are 95%. The interference efficiency on all beam-splitters are about 99%.

Preparation and verification of the square cluster state

The four-mode entangled state used in the experiment is a continuous variable (CV) square Gaussian cluster state of optical field at the sideband frequency of 3 MHz and is prepared by coupling two phase-squeezed and two amplitude-squeezed states of light on an optical beam-splitter network, which consists of three optical beam-splitters with transmit-

tance of $T_1 = 1/5$ and $T_2 = T_3 = 1/2$, respectively, as shown in Fig. 1(b) in the main text. Four input squeezed states are expressed by

$$\begin{aligned}\hat{a}_1 &= \frac{1}{2}[e^{r_1}\hat{x}_1^{(0)} + ie^{-r_1}\hat{p}_1^{(0)}], \\ \hat{a}_2 &= \frac{1}{2}[e^{-r_2}\hat{x}_2^{(0)} + ie^{r_2}\hat{p}_2^{(0)}], \\ \hat{a}_3 &= \frac{1}{2}[e^{-r_3}\hat{x}_3^{(0)} + ie^{r_3}\hat{p}_3^{(0)}], \\ \hat{a}_4 &= \frac{1}{2}[e^{r_4}\hat{x}_4^{(0)} + ie^{-r_4}\hat{p}_4^{(0)}],\end{aligned}\quad (6)$$

where r_i ($i = 1, 2, 3, 4$) is the squeezing parameter, $\hat{x} = \hat{a} + \hat{a}^\dagger$ and $\hat{p} = (\hat{a} - \hat{a}^\dagger)/i$ are the amplitude and phase quadratures of an optical field \hat{a} , respectively, and the superscript of the amplitude and phase quadratures represent the vacuum state. The transformation matrix of the beam-splitter network is given by

$$U = \begin{bmatrix} -\sqrt{\frac{1}{2}} & -\sqrt{\frac{2}{5}} & -\frac{i}{\sqrt{10}} & 0 \\ \sqrt{\frac{1}{2}} & -\sqrt{\frac{2}{5}} & -\frac{i}{\sqrt{10}} & 0 \\ 0 & \frac{i}{\sqrt{10}} & \sqrt{\frac{2}{5}} & -\sqrt{\frac{1}{2}} \\ 0 & \frac{i}{\sqrt{10}} & \sqrt{\frac{2}{5}} & \sqrt{\frac{1}{2}} \end{bmatrix}, \quad (7)$$

the unitary matrix can be decomposed into a beam-splitter network $U = F_4 F_3 I_1(-1) B_{34}(T_3) F_4 B_{12}(T_2) B_{23}(T_1) F_3$, where $B_{kl}(T_j)$ stands for the linearly optical transformation on j th beam-splitter with transmission of T_j ($j = 1, 2, 3$), where $(B_{kl})_{kk} = \sqrt{1-T}$, $(B_{kl})_{kl} = (B_{kl})_{lk} = \sqrt{T}$, $(B_{kl})_{ll} = -\sqrt{1-T}$ ($k, l = 1, 2, 3, 4$), are matrix elements of the beam-splitter. $F_k [I_k(-1)]$ denotes the 90° (180°) rotation in phase space of mode k , $\hat{a}_k \rightarrow i\hat{a}_k$ ($\hat{a}_k \rightarrow -\hat{a}_k$). The output modes from the optical beam-splitter network are expressed by

$$\begin{aligned}\hat{A} &= -\sqrt{\frac{1}{2}}\hat{a}_1 - \sqrt{\frac{2}{5}}\hat{a}_2 - i\sqrt{\frac{1}{10}}\hat{a}_3, \\ \hat{B} &= \sqrt{\frac{1}{2}}\hat{a}_1 - \sqrt{\frac{2}{5}}\hat{a}_2 - i\sqrt{\frac{1}{10}}\hat{a}_3, \\ \hat{C} &= i\sqrt{\frac{1}{10}}\hat{a}_2 + \sqrt{\frac{2}{5}}\hat{a}_3 - \sqrt{\frac{1}{2}}\hat{a}_4, \\ \hat{D} &= i\sqrt{\frac{1}{10}}\hat{a}_2 + \sqrt{\frac{2}{5}}\hat{a}_3 + \sqrt{\frac{1}{2}}\hat{a}_4,\end{aligned}\quad (8)$$

respectively. Here, we have assumed that four squeezed states have the identical squeezing parameter ($r_1 = r_2 = r_3 = r_4$). In experiments, the requirement is easily achieved by adjusting the two NOPAs to operate precisely at the same conditions. For our experimental system, we have measured $r = 0.345$. The quantum correlations between the amplitude and phase quadratures are expressed by $\Delta^2(\hat{p}_A - \hat{x}_C - \hat{x}_D) = \Delta^2(\hat{p}_B - \hat{x}_C - \hat{x}_D) = \Delta^2(\hat{p}_C - \hat{x}_A - \hat{x}_B) = \Delta^2(\hat{p}_D - \hat{x}_A - \hat{x}_B) = 3e^{-2r}$, where the subscripts correspond to different optical modes. Obviously, in the ideal case with infinite squeezing ($r \rightarrow \infty$), these noise variances will vanish and the better the squeezing, the smaller the noise terms.

According to the criteria for CV multipartite entanglement proposed by van Loock and Furusawa [65], we deduce the inseparability conditions for the CV four-mode square cluster state, which are

$$\begin{aligned} \Delta^2(\hat{p}_A - \hat{x}_C - \hat{x}_D) + \Delta^2(\hat{p}_C - \hat{x}_A - \hat{x}_B) &< 4, \\ \Delta^2(\hat{p}_A - \hat{x}_C - \hat{x}_D) + \Delta^2(\hat{p}_D - \hat{x}_A - \hat{x}_B) &< 4, \\ \Delta^2(\hat{p}_B - \hat{x}_C - \hat{x}_D) + \Delta^2(\hat{p}_C - \hat{x}_A - \hat{x}_B) &< 4, \\ \Delta^2(\hat{p}_B - \hat{x}_C - \hat{x}_D) + \Delta^2(\hat{p}_D - \hat{x}_A - \hat{x}_B) &< 4. \end{aligned} \quad (9)$$

When all the combinations of variances of nullifiers in the left-hand sides of these inequalities are smaller than 4 (which defines the normalized boundary for inseparability, given a unit variance for each quadrature of the vacuum state), then the four modes are in a fully inseparable CV square cluster state.

The correlation variances measured experimentally are shown in Fig. S1. They are $\Delta^2(\hat{p}_A - \hat{x}_C - \hat{x}_D) = -2.84 \pm 0.20$ dB, $\Delta^2(\hat{p}_B - \hat{x}_C - \hat{x}_D) = -2.97 \pm 0.19$ dB, $\Delta^2(\hat{p}_C - \hat{x}_A - \hat{x}_B) = -2.97 \pm 0.19$ dB and $\Delta^2(\hat{p}_D - \hat{x}_A - \hat{x}_B) = -3.05 \pm 0.19$ dB, respectively. From these measured results we can calculate the combinations of the correlation variances in the left-hand sides of the inequalities (9),¹ which are 3.07 ± 0.02 , 3.05 ± 0.02 , 3.03 ± 0.02 and 3.01 ± 0.02 , respectively. Thus all inequalities (9) are simultaneously satisfied, which confirms the prepared state is a fully inseparable CV four-mode square cluster state.

MEASUREMENT OF THE COVARIANCE MATRIX

A Gaussian state is a state with Gaussian characteristic functions and quasi-probability distributions on the multi-mode quantum phase space, which can be completely characterized by its covariance matrix. The elements of the covariance matrix are $\sigma_{ij} = \text{Cov}(\hat{\xi}_i, \hat{\xi}_j) = \frac{1}{2} \langle \hat{\xi}_i \hat{\xi}_j + \hat{\xi}_j \hat{\xi}_i \rangle - \langle \hat{\xi}_i \rangle \langle \hat{\xi}_j \rangle$, $i, j = 1, 2, \dots, 8$, where $\hat{\xi} = (\hat{x}_A, \hat{p}_A, \hat{x}_B, \hat{p}_B, \hat{x}_C, \hat{p}_C, \hat{x}_D, \hat{p}_D)^T$ is a vector composed by the amplitude and phase quadratures of four-mode states [64]. For convenience, the covariance matrix of the original four-mode Gaussian state is written in terms of two-by-two submatrices as

$$\sigma = \begin{bmatrix} \sigma_A & \sigma_{AB} & \sigma_{AC} & \sigma_{AD} \\ \sigma_{AB}^T & \sigma_B & \sigma_{BC} & \sigma_{BD} \\ \sigma_{AC}^T & \sigma_{BC}^T & \sigma_C & \sigma_{CD} \\ \sigma_{AD}^T & \sigma_{BD}^T & \sigma_{CD}^T & \sigma_D \end{bmatrix}, \quad (10)$$

Thus the four-mode covariance matrix can be partially expressed as (the cross correlations between different quadratures of one mode are taken as 0)

$$\begin{aligned} \sigma_A &= \begin{bmatrix} \Delta^2 \hat{x}_A & 0 \\ 0 & \Delta^2 \hat{p}_A \end{bmatrix}, \\ \sigma_B &= \begin{bmatrix} \Delta^2 \hat{x}_B & 0 \\ 0 & \Delta^2 \hat{p}_B \end{bmatrix}, \\ \sigma_C &= \begin{bmatrix} \Delta^2 \hat{x}_C & 0 \\ 0 & \Delta^2 \hat{p}_C \end{bmatrix}, \\ \sigma_D &= \begin{bmatrix} \Delta^2 \hat{x}_D & 0 \\ 0 & \Delta^2 \hat{p}_D \end{bmatrix}, \\ \sigma_{AB} &= \begin{bmatrix} \text{Cov}(\hat{x}_A, \hat{x}_B) & \text{Cov}(\hat{x}_A, \hat{p}_B) \\ \text{Cov}(\hat{p}_A, \hat{x}_B) & \text{Cov}(\hat{p}_A, \hat{p}_B) \end{bmatrix}, \\ \sigma_{AC} &= \begin{bmatrix} \text{Cov}(\hat{x}_A, \hat{x}_C) & \text{Cov}(\hat{x}_A, \hat{p}_C) \\ \text{Cov}(\hat{p}_A, \hat{x}_C) & \text{Cov}(\hat{p}_A, \hat{p}_C) \end{bmatrix}, \\ \sigma_{AD} &= \begin{bmatrix} \text{Cov}(\hat{x}_A, \hat{x}_D) & \text{Cov}(\hat{x}_A, \hat{p}_D) \\ \text{Cov}(\hat{p}_A, \hat{x}_D) & \text{Cov}(\hat{p}_A, \hat{p}_D) \end{bmatrix}, \\ \sigma_{BC} &= \begin{bmatrix} \text{Cov}(\hat{x}_B, \hat{x}_C) & \text{Cov}(\hat{x}_B, \hat{p}_C) \\ \text{Cov}(\hat{p}_B, \hat{x}_C) & \text{Cov}(\hat{p}_B, \hat{p}_C) \end{bmatrix}, \\ \sigma_{BD} &= \begin{bmatrix} \text{Cov}(\hat{x}_B, \hat{x}_D) & \text{Cov}(\hat{x}_B, \hat{p}_D) \\ \text{Cov}(\hat{p}_B, \hat{x}_D) & \text{Cov}(\hat{p}_B, \hat{p}_D) \end{bmatrix}, \\ \sigma_{CD} &= \begin{bmatrix} \text{Cov}(\hat{x}_C, \hat{x}_D) & \text{Cov}(\hat{x}_C, \hat{p}_D) \\ \text{Cov}(\hat{p}_C, \hat{x}_D) & \text{Cov}(\hat{p}_C, \hat{p}_D) \end{bmatrix}. \end{aligned} \quad (11)$$

From the output modes given in Eq. (8) and the information of the four input squeezed states given in Eq. (6), we can theoretically obtain the amplitude and phase quadratures of the four-mode state and then determine all the elements of the covariance matrix in Eq. 10. These are used for the theoretical predictions.

In the experiment, to partially reconstruct all relevant entries of the associated covariance matrix of the state, we perform 32 different measurements on the output optical modes. These measurements include the amplitude and phase quadratures of the output optical modes, and the cross correlations $\Delta^2(\hat{x}_A - \hat{x}_B)$, $\Delta^2(\hat{x}_A - \hat{x}_C)$, $\Delta^2(\hat{x}_A - \hat{x}_D)$, $\Delta^2(\hat{x}_B - \hat{x}_C)$, $\Delta^2(\hat{x}_B - \hat{x}_D)$, $\Delta^2(\hat{x}_C - \hat{x}_D)$, $\Delta^2(\hat{p}_A - \hat{p}_B)$, $\Delta^2(\hat{p}_A - \hat{p}_C)$, $\Delta^2(\hat{p}_A - \hat{p}_D)$, $\Delta^2(\hat{p}_B - \hat{p}_C)$, $\Delta^2(\hat{p}_B - \hat{p}_D)$, $\Delta^2(\hat{p}_C - \hat{p}_D)$, $\Delta^2(\hat{x}_A + \hat{p}_B)$, $\Delta^2(\hat{x}_A + \hat{p}_C)$, $\Delta^2(\hat{x}_A + \hat{p}_D)$, $\Delta^2(\hat{x}_B + \hat{p}_C)$, $\Delta^2(\hat{x}_B + \hat{p}_D)$, $\Delta^2(\hat{x}_C + \hat{p}_D)$, $\Delta^2(\hat{p}_A + \hat{x}_B)$, $\Delta^2(\hat{p}_A + \hat{x}_C)$, $\Delta^2(\hat{p}_A + \hat{x}_D)$, $\Delta^2(\hat{p}_B + \hat{x}_C)$, $\Delta^2(\hat{p}_B + \hat{x}_D)$ and $\Delta^2(\hat{p}_C + \hat{x}_D)$. The covariance elements are calculated via the identities [66]

$$\begin{aligned} \text{Cov}(\hat{\xi}_i, \hat{\xi}_j) &= \frac{1}{2} \left[\Delta^2(\hat{\xi}_i + \hat{\xi}_j) - \Delta^2 \hat{\xi}_i - \Delta^2 \hat{\xi}_j \right], \\ \text{Cov}(\hat{\xi}_i, \hat{\xi}_j) &= -\frac{1}{2} \left[\Delta^2(\hat{\xi}_i - \hat{\xi}_j) - \Delta^2 \hat{\xi}_i - \Delta^2 \hat{\xi}_j \right]. \end{aligned} \quad (12)$$

The steerability of Bob by Alice ($A \rightarrow B$) for a $(n_A + n_B)$ -mode Gaussian state under Gaussian measurements can be quantified by Eq. (3) in the main text, based on the symplectic eigenvalues derived from the Schur complement of A in the covariance matrix. In Figs. 2–4 of the main text and Figs. 2–3,

¹ Note that the experimental variances are measured in dB. To insert the values into the inequalities (9), we need to convert them back into dimensionless units, via the formula: $\Delta^2(\hat{p}_i - \hat{x}_j - \hat{x}_k) = 3 \times 10^{(\text{variance in dB})/10}$.

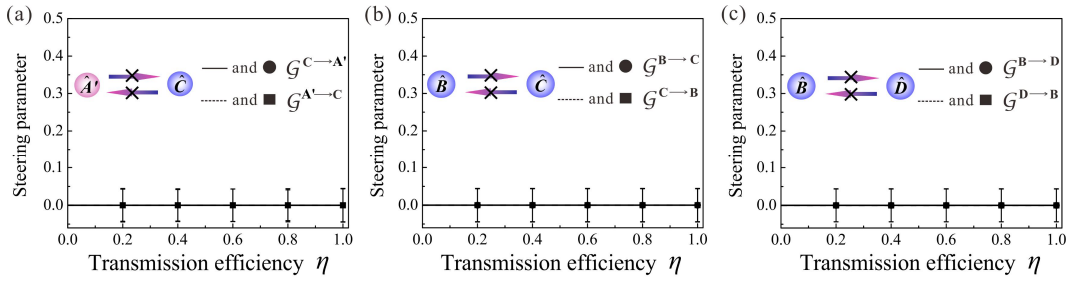


FIG. 2: Gaussian EPR steering between two modes of the cluster state, supplementing Fig. 2 in the main text. (a)–(c) Gaussian EPR steering between neighboring modes \hat{A}' and \hat{C} , \hat{C} and \hat{B} , \hat{B} and \hat{D} , respectively. Clearly, no EPR steering is possible between these (1+1)-mode neighboring modes in the CV four-mode square Gaussian cluster state under Gaussian measurements. In all the panels, the quantities plotted are dimensionless. The lines and curves represent theoretical predictions. The dots and squares represent the experimental data measured at different transmission efficiencies. Error bars represent \pm one standard deviation and are obtained based on the statistics of the measured noise variances.

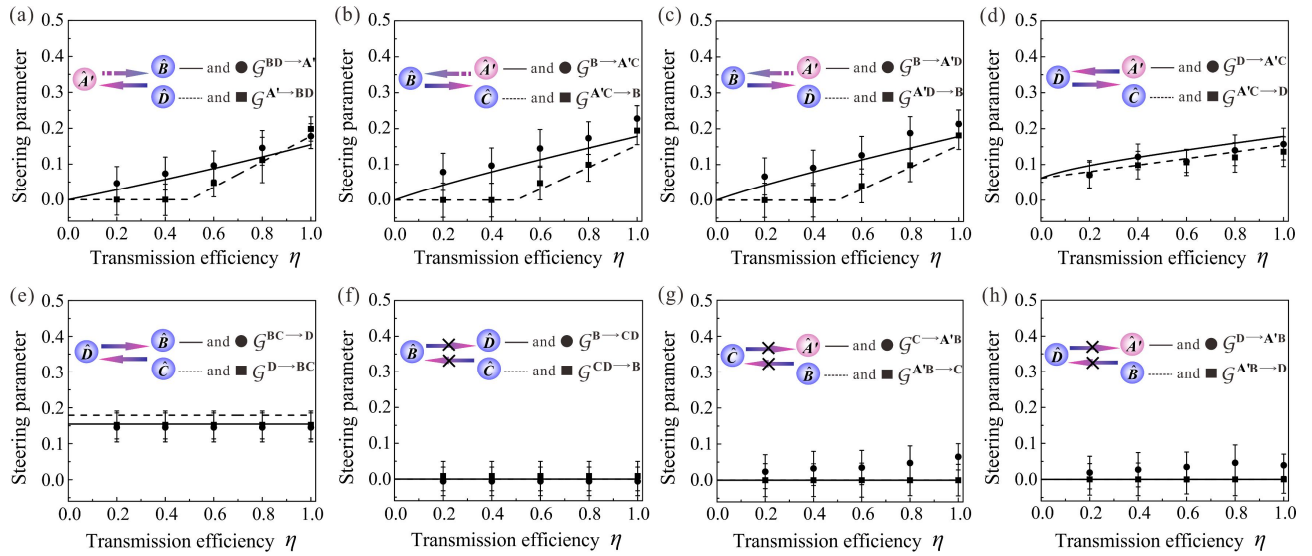


FIG. 3: Gaussian EPR steering between one and two modes of the cluster state, supplementing Fig. 3 in the main text. (a) One-way EPR steering between modes \hat{A}' and $\{\hat{B}$ and $\hat{C}\}$ under Gaussian measurements. (b) One-way EPR steering between modes \hat{B} and $\{\hat{A}'$ and $\hat{C}\}$ under Gaussian measurements. (c) One-way EPR steering between modes \hat{B} and $\{\hat{A}'$ and $\hat{D}\}$ under Gaussian measurements. (d) \hat{D} and $\{\hat{A}'$ and $\hat{C}\}$ can steer each other asymmetrically and the Gaussian steerability grows with the increasing transmission efficiency. (e) \hat{D} and $\{\hat{B}$ and $\hat{C}\}$ can steer each other asymmetrically. (f) There is no EPR steering between \hat{B} and $\{\hat{C}$ and $\hat{D}\}$ under Gaussian measurements. (g) There is no EPR steering between \hat{C} and $\{\hat{A}'$ and $\hat{B}\}$ under Gaussian measurements. (h) There is no EPR steering between \hat{D} and $\{\hat{A}'$ and $\hat{B}\}$ under Gaussian measurements. In all the panels, the quantities plotted are dimensionless. The lines and curves represent theoretical predictions. The dots and squares represent the experimental data measured at different transmission efficiencies. Error bars represent \pm one standard deviation and are obtained based on the statistics of the measured noise variances.

the lines and curves represent theoretical predictions based on the theoretically calculated covariance matrix, while the dots and squares report the measured steerability as evaluated from the experimentally reconstructed covariance matrix.

SUPPLEMENTARY FIGURES

In this section, we provide additional figures that supplement the main text. In particular, the additional experimental results of EPR steering between neighboring modes \hat{A}' and \hat{C} , \hat{B} and \hat{C} , \hat{B} and \hat{D} under Gaussian measurements are shown in Fig. 2, which supplements Fig. 2 in the main text. These

figures support the result that no steering exist between neighboring modes in the four-mode square Gaussian cluster entangled state under Gaussian measurements.

We also provide the additional experimental results of EPR steering between one and two modes [(1+2)-mode and (2+1)-mode partitions] of the CV four-mode square cluster state under Gaussian measurements. The results of \hat{A}' and $\{\hat{B}$ and $\hat{C}\}$, \hat{B} and $\{\hat{A}'$ and $\hat{C}\}$, \hat{B} and $\{\hat{A}'$ and $\hat{D}\}$, \hat{D} and $\{\hat{A}'$ and $\hat{C}\}$, \hat{D} and $\{\hat{B}$ and $\hat{C}\}$, \hat{B} and $\{\hat{C}$ and $\hat{D}\}$, \hat{C} and $\{\hat{A}'$ and $\hat{B}\}$, \hat{D} and $\{\hat{A}'$ and $\hat{B}\}$ are shown in Fig. 3, which supplements Fig. 3 in the main text. All the results provide complete support to our analysis and conclusions as discussed in the main text.